Spatial survival probability for one-dimensional fluctuating interfaces in the steady state

Satya N. Majumdar
Laboratoire de Physique Theorique et Modeles Statistiques, Universite Paris-Sud, Bat. 100, 91405 ORSAY cedex, France

Chandan Dasgupta
Centre for Condensed Matter Theory, Department of Physics, Indian Institute of Science, Bangalore 560012, India
(Received 31 August 2005; revised manuscript received 24 October 2005; published 9 January 2006)

We report numerical and analytic results for the spatial survival probability for fluctuating one-dimensional interfaces with Edwards-Wilkinson or Kardar-Parisi-Zhang dynamics in the steady state. Our numerical results are obtained from analysis of steady-state profiles generated by integrating a spatially discretized form of the Edwards-Wilkinson equation to long times. We show that the survival probability exhibits scaling behavior in its dependence on the system size and the "sampling interval" used in the measurement for both "steady-state" and "finite" initial conditions. Analytic results for the scaling functions are obtained from a path-integral treatment of a formulation of the problem in terms of one-dimensional Brownian motion. A "deterministic approximation" is used to obtain closed-form expressions for survival probabilities from the formally exact analytic treatment. The resulting approximate analytic results provide a fairly good description of the numerical data.

DOI: 10.1103/PhysRevE.73.011602 PACS number(s): 68.37.Ef, 68.35.Ja, 05.20.−y

I. INTRODUCTION

Temporal first-passage properties, expressed in terms of persistence and survival probabilities [1], have recently found many applications [2–5] in the study of the dynamics of fluctuating interfaces. Experimental realizations of one-dimensional (1D) fluctuating interfaces are provided by monatomic steps on vicinal surfaces. Recent experimental studies [6–9] have shown that temporal persistence and survival probabilities for fluctuating steps can be measured, and that these probabilities provide a convenient way of characterizing their dynamics. The temporal persistence probability is defined in this context as the probability that the height at a particular point of the interface does not return to its *initial value* over a certain period of time. For many simple models of interface dynamics, this probability exhibits a power-law decay in time [2–4]. This power-law behavior has been confirmed in experiments [6–9]. In contrast, a closely related quantity, the temporal survival probability that measures the probability that the height does not return to its *average value* over a certain period of time is found, both theoretically [5] and experimentally [8,9], to decay exponentially at long times.

In studies of fluctuating interfaces, it is natural to consider spatial analogs of these temporal first-passage quantities, namely the *spatial persistence and survival probabilities*. These probabilities have been studied analytically [10] and numerically [11] for several models of interfacial dynamics. For $(1+1)$-dimensional interfaces, the stochastic variable of interest is the "height" $h(x,t)$ that represents the position of the interface at point x and time t. In this paper, we consider the interface profile $h(x,t_0)$ where the time t_0 is in the long-time, steady-state regime and, for notational convenience, suppress the time argument t_0 of h from now on. To define spatial persistence probabilities, let $p(x_0,x_0+x)$ be the probability that the height $h(x)$ *does not* return to its "initial" value $h(x_0)$ at the point x_0 within a distance x measured from x_0 along the interface. The "steady-state" spatial persistence probability $P(x)$ is then defined as the average of $p(x_0,x_0+x)$ over *all* possible choices of the initial point x_0 in a steady-state configuration of the interface. A second persistence probability $P_{FIC}(x)$, the so-called spatial persistence probability for "finite initial conditions" (FIC) [10], is defined as the average of $p(x_0,x_0+x)$ over initial points x_0 at which both the height $h(x_0)$ and its spatial derivative $h'(x_0)$ are finite. It was shown in Refs. [10,11] that for several models of fluctuating interfaces, both $P(x)$ and $P_{FIC}(x)$ exhibit power-law decay for large x, but the exponents that describe this power-law behavior may be different in the two cases. Experimental measurements of the steady-state spatial persistence probability for interfaces (combustion fronts in paper) believed to be described by the Kardar-Parisi-Zhang (KPZ) equation [12] have been reported recently [13]. The behavior of $P_{FIC}(x)$ was not investigated in this work.

In analogy with the temporal case, the *spatial survival probabilities* are defined in terms of the probability $p'(x_0,x_0+x)$ that the interface height between points x_0 and x_0+x does not cross its *average value* $\bar{h}$ [rather than the initial value $h(x_0)$]. The steady-state and FIC spatial survival probabilities, $Q(x)$ and $Q_{FIC}(x)$, respectively, are then obtained by averaging $p'(x_0,x_0+x)$ over x_0 in the two different ways mentioned above: in the first case, the average is done over all points x_0, while, in the second case, the average is performed over only the points at which the height and its spatial derivative are finite. Numerical results for the x dependence of these two spatial survival probabilities for 1D interfaces with KPZ and Edwards-Wilkinson (EW) [14] dynamics were reported in Ref. [11]. It was found there that the spatial dependence of $Q(x)$ is neither power law nor exponential, while $Q_{FIC}(x)$ exhibits a power-law decay similar to that of the FIC persistence probability $P_{FIC}(x)$. While the power-law behavior of $Q_{FIC}(x)$ was expected [10], the x de-

 ©2006 The American Physical Society

pendence of $Q(x)$ found in the numerical work of Ref. [11] was not understood theoretically.

In this paper, we present the results of a detailed numerical and analytic study of the spatial survival probabilities for 1D interfaces with EW dynamics in the steady state. The primary motivation for this study is to develop a theoretical understanding of the numerical results reported in Ref. [11]. On a more general level, studies of temporal and spatial first-passage properties of fluctuating interfaces are believed to be important in understanding the role of thermal fluctuations of the edges of components in the stability of nano-scale devices. The 1D EW equation is believed [15] to describe thermal fluctuations of steps on a vicinal surface under experimental conditions for which the dominant source of fluctuations is the attachment/detachment of atoms to/from the steps. Since the statistics of height fluctuations in the steady state of the 1D KPZ equation is the same as that for the 1D EW equation, our results also apply to experimental realizations of 1D KPZ interfaces.

The 1D EW equation has the form [14]

$$\frac{\partial h(x,t)}{\partial t} = \Gamma \frac{\partial^2 h(x,t)}{\partial x^2} + \eta(x,t), \tag{1}$$

where Γ is a kinetic parameter and $\eta(x,t)$ is a Gaussian random noise with $\langle \eta(x,t)\rangle = 0$, $\langle \eta(x,t)\eta(x',t')\rangle = 2D'\delta(x-x')\delta(t-t')$, D' being a measure of the strength of the noise. The parameters Γ and D' should satisfy the fluctuation-dissipation relation if this equation is supposed to describe equilibrium fluctuations (e.g., in the case of steps on a vicinal surface), but they are independent parameters in a general nonequilibrium situation. We consider a finite system of size L, so that $0 \leqslant x \leqslant L$, and use periodic boundary conditions. It is easy to see that the spatial average $\bar{h}(t) \equiv (1/L)\int_0^L h(x,t)dx$ executes a simple random walk in time. In our calculations, we subtract the spatial average from the variables $h(x,t)$, so that, from now on, it is implied that $h(x,t)$ represents the height at point x measured from the instantaneous spatial average. Thus, $\bar{h}(t)$ is equal to zero by definition. As we shall see later, this condition plays an important role in the analytic calculation.

The spatial survival probabilities studied here are defined as follows. Let $Q(x,L|h_0)$ denote the probability that the steady-state spatial profile of the interface starting at h_0 at $x=0$ (and ending at h_0 at $x=L$, i.e., with periodic boundary condition) does not cross 0 up to a distance x where $0 \leqslant x \leqslant L$. Then, the steady-state spatial survival probability is given by

$$Q(x,L) = \int_{-\infty}^{\infty} Q(x,L|h_0) P_{st}(h_0,L) dh_0, \tag{2}$$

where $P_{st}(h_0,L)$ is the steady-state height distribution. The FIC survival probability is defined as

$$Q_{FIC}(x,L,w) = \frac{\int_{-w}^{w} Q(x,L|h_0) P_{st}(h_0,L) dh_0}{\int_{-w}^{w} P_{st}(h_0,L) dh_0}, \tag{3}$$

where $w \ll W(L)$, the steady-state width of the interface. In our numerical work, steady-state profiles for systems of different L are generated by integrating a spatially discretized form of the EW equation to long times, and these profiles are used to calculate the survival probabilities. The spatial discretization implies that there is a finite *sampling interval* δx that represents the spacing between successive points at which the height variable is sampled in the calculation of the survival probabilities. Clearly, the value of δx must be an integral multiple of the spacing of the spatial grid at which the height variable is defined. This sampling interval δx is analogous to the "sampling time" that represents the interval between two successive measurements of a stochastic process in studies of temporal persistence. The fact that a finite value of the "sampling time" may modify the persistence properties of a stationary stochastic process was first pointed out in Ref. [16]. In the context of fluctuating interfaces, it is known from numerical [4,5] and experimental [9] studies that the temporal survival probability in interfaces exhibits a nontrivial dependence on the sampling time. In our numerical study, we find that the spatial survival probabilities also depend on the value of the sampling interval δx. The dependence of the survival probability Q on x, L, and δx is found to be described by a scaling function of x/L and $\delta x/L$: $Q(x,L,\delta x) = f_d(x/L, \delta x/L)$. This is similar to the scaling behavior found in Ref. [11] for spatial persistence probabilities. As shown there, the dependence of the FIC survival probability Q_{FIC} on x, L, δx, and w is also described by a scaling function of x/L, $\delta x/L$, and w/L^{α} where $\alpha = 0.5$ is the exponent for the dependence of the steady-state width $W(L)$ on L [$W(L) \propto L^{\alpha}$].

In our analytic study, we consider the spatial survival probabilities when the height variable is sampled continuously, i.e., the limit $\delta x \to 0$, and calculate the scaling function $f(x/L) \equiv f_d(x/L, 0)$. This calculation is based on a mapping of the spatial statistics of a steady-state EW interface to the temporal statistics of 1D Brownian motion. The requirement that the average height $\bar{h}$ of the interface must vanish translates in this mapping to the constraint that the total area under the curve that represents the Brownian process in the distance-time plane must be zero. This "zero-area" constraint plays a very important role in the analytic calculation—the form of the scaling function $f(u)$ depends crucially on whether this constraint is imposed in the analytic treatment. Without this constraint, we can determine $f(u)$ exactly, but the form of the scaling function obtained this way differs drastically from the numerical result. In particular, the scaling function does not go to zero as $u \to 1$, whereas the numerically obtained scaling function decreases rather fast to 0 as u approaches 1. When we take into account the zero-area global constraint, determining the scaling function $f(u)$ analytically becomes much more nontrivial. We are able to set

up an exact path integral technique that allows us, in principle, to compute this function exactly in terms of some complicated integrals. However, we cannot get an exact closed form expression for $f(u)$ to compare with the simulation data. We then make a simple "deterministic" approximation that allows us to obtain a a closed form expression for $f(u)$ which we then compare with the numerically obtained scaling function. The agreement is fairly good, given the drastic nature of the deterministic approximation. Our approximate analytic result for the FIC survival probability also shows similar agreement with the numerically obtained results.

The rest of this paper is organized as follows. In Sec. II, we describe our numerical results for the spatial survival probabilities. The analytic calculations with and without the "zero-area" constraint are described in detail in Sec. III. In this section, we also present a comparison of the analytic results for the survival probabilities with the numerical results presented in Sec. II. Section IV contains a summary of the main results and a few concluding remarks. Some details of the steady-state properties of finite 1D EW interfaces with periodic boundary conditions are presented in the Appendix.

II. NUMERICAL RESULTS

In the numerical work, we consider a spatially discretized dimensionless form of the 1D EW equation defined in Eq. (1). The height variable is defined on a 1D lattice of unit spacing with periodic boundary conditions. Let h_i be the height at lattice site i with $i=1,2,\ldots,L$. The time dependence of the height variables is given by

$$\frac{dh_i(t)}{dt} = [h_{i+1}(t) - 2h_i(t) + h_{i-1}(t)] + \eta_i(t), \tag{4}$$

where the $\eta_i(t)$'s represent uncorrelated Gaussian noise with $\langle \eta_i(t)\rangle = 0$ and $\langle \eta_i(t)\,\eta_j(t')\rangle = 2\delta_{ij}\delta(t-t')$. Equation (4) is thus a discretized version of the continuum EW equation (1) with the choice $\Gamma=1$ and $D'=1$. These equations are integrated forward in time using the simple Euler method [17]. Thus, we write Eq. (4) as

$$h_i(t+\delta t) - h_i(t) = \delta t[h_{i+1}(t) - 2h_i(t) + h_{i-1}(t)] + \sqrt{\delta t}\, r_i(t), \tag{5}$$

where each $r_i(t)$ is an independent Gaussian random number of zero mean and variance equal to 2. We use a value of δt small enough (i.e., $\delta t = 0.01$) to avoid any numerical instability. Steady-state interface profiles are generated by carrying out the integration from flat initial states ($h_i=0$ for all i) to sufficiently long times (much longer than the time at which the width of the interface saturates). As mentioned in Sec. I, we always subtract the instantaneous spatial average of the height variables from the individual variables $\{h_i\}$ so that the condition $\Sigma_{i=1}^{L} h_i = 0$ is always satisfied.

The steady-state spatial survival probability $Q(x)$ is measured as the probability that the interface height variable does not cross zero as one moves along the interface from an initial point x_0 to the point x_0+x (since the height variables are defined on a lattice of unit spacing, both x_0 and x are integers between 0 and L.) This probability is averaged over all initial points x_0 in a steady-state configuration and also over many (typically 10^4) independent realizations of the stochastic evolution that generates the steady-state profiles. The minimum value of the sampling interval δx used in the measurement of $Q(x)$ is obviously the lattice spacing which is equal to unity. However, it is also possible to use a larger sampling interval, equal to a positive integer m, in the measurement of $Q(x)$—this is done by considering only the heights at the lattice sites $i=km$, $k=1,2,\ldots$, while checking whether the height crosses zero between the points x_0 and x_0+x. The measured survival probability exhibits a weak dependence on the value of δx. The FIC survival probability is measured in a similar way, except that the initial points x_0 are chosen to be only those at which the height lies between $-w$ and $+w$, with $w \ll W(L)$, the steady-state width of the interface.

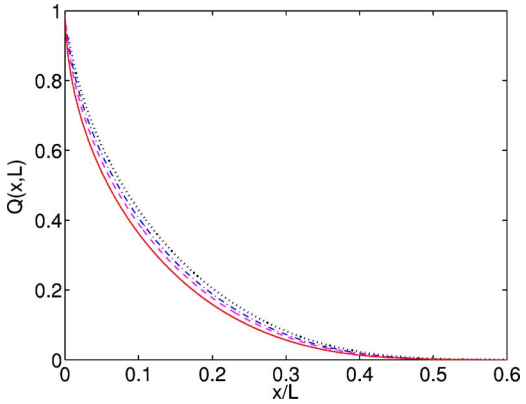

FIG. 1. (Color online) Plots of the spatial survival probability $Q(x,L)$ as a function of x/L (L is the sample size) for $L=200$ [(black) dotted line], $L=400$ [(blue) dash-dotted line], $L=800$ [(magenta) dashed line], and $L=10^4$ [(red) full line]. The same sampling interval, $\delta x=1$, is used in all cases.

Typical results for the survival probability $Q(x)$ are shown in Figs. 1–4. In Fig. 1, we show plots of $Q(x)$ as a function of x/L for $L=200$, 400, and 800. The values of $Q(x)$ shown

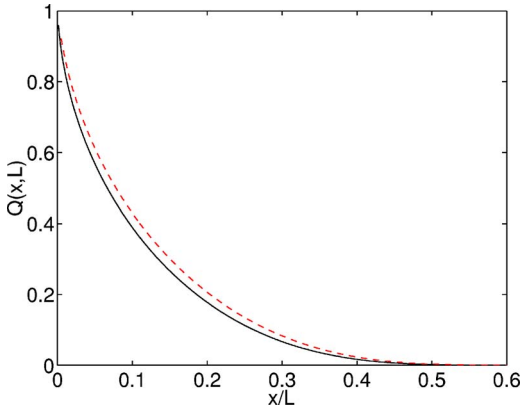

FIG. 2. (Color online) Dependence of the spatial survival probability on the sampling interval δx used in its measurement. Plots of $Q(x,L)$ versus x/L (L is the sample size) are shown for $L=800$, and two values of δx: $\delta x=1$ [(black) full line] and $\delta x=4$ [(red) dashed line].

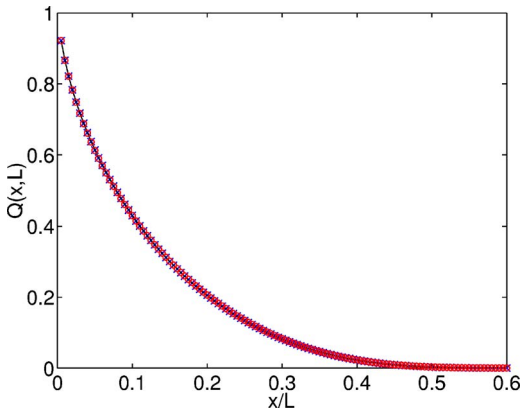

FIG. 3. (Color online) The scaling behavior [Eq. (6)] of the dependence of the spatial survival probability on the sample size L and the sampling interval δx. Plots of $Q(x,L)$ versus x/L are shown for three different sets of values of L and δx with $\delta x/L$ held constant: $L=200$ and $\delta x=1$ [(blue) crosses]; $L=400$ and $\delta x=2$ [(black) line]; $L=800$ and $\delta x=4$ [(red) circles].

in these plots were obtained using $\delta x=1$ (unless mentioned otherwise, all the results shown here were obtained using this "default" value of δx). It is clear from the plots that $Q(x)$ decreases from 1 to a value close to 0 as x/L is increased from 0 to about 0.6. The numerical results show a weak dependence on the value of L. As we shall see shortly, this dependence arises from the use of the same δx in all the measurements for the different values of L.

The numerical calculations cannot be extended to much larger values of L because the time required to reach the steady state from a flat initial state increases with L as L^z with $z=2$. However, we have found a different way of generating steady-state interface profiles for much larger values of L. It is easy to show that in the steady state of the model defined in Eq. (4), the height difference variables $s_i \equiv h_{i+1}-h_i$, $i=1,2,\ldots,L$ (with $h_{L+1}=h_1$ due to periodic boundary conditions) are independent Gaussian random variables with zero mean and variance equal to unity, apart from the obvious constraint, $\Sigma_{i=1}^{L} s_i=0$, arising from periodic

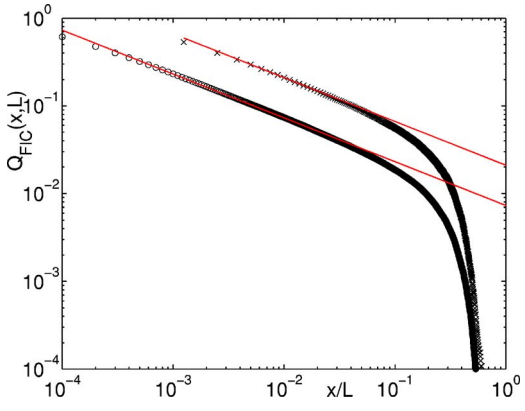

FIG. 4. (Color online) Double-log plots of the FIC spatial survival probability $Q_{FIC}(x,L)$ versus x/L (L is the sample size) for $L=800$ (crosses) and $L=10^4$ (circles). Fits of the initial decay of Q_{FIC} to a power-law with exponent $\frac{1}{2}$ [$Q_{FIC}(x) \propto x^{-0.5}$] are shown by the (red) solid lines.

boundary conditions. Therefore, a realization of the steady-state interface profile for a system of size L may be obtained by numerically generating L Gaussian random variables with the statistics mentioned above, identifying these random variables with the s_i's, and then calculating the heights h_i (with their spatial average subtracted off) in terms of these s_i's. We have calculated the spatial survival probabilities for steady-state EW interfaces with $L=10^4$ generated this way, averaging over 4000 independent realizations. The results for $Q(x)$ obtained from this calculation are also shown in Fig. 1. It is clear that these results for $L=10^4$ are consistent with the trend shown by the other results obtained from steady-state interfaces generated by numerical integration.

In Fig. 2, we have shown plots of $Q(x)$ for $L=800$, obtained from two different calculations, one with $\delta x=1$ and the other with $\delta x=4$. The two curves are clearly different, indicating that the measured $Q(x)$ depends weakly on the value of δx used in the measurement. We have found, in analogy with the results reported in Ref. [11] for spatial persistence probabilities, that the dependence of Q on x, L, and δx satisfies the scaling equation

$$Q(x,L,\delta x) = f_d(x/L, \delta x/L), \tag{6}$$

where the subscript "d" of the scaling function is meant to indicate that here we are considering survival probabilities measured using discrete sampling with a finite sampling interval δx. This scaling equation implies that plots of $Q(x)$ vs. x/L for samples with different L would all collapse to the same curve if the survival probabilities for different L are measured using different values of δx, such that $\delta x/L$ is held constant. This scaling behavior is illustrated in Fig. 3. In this figure, we have shown plots of Q vs. x/L for $L=200$ measured with $\delta x=1$, $L=400$ measured with $\delta x=2$, and $L=800$ measured with $\delta x=4$ (so that $\delta x/L=\frac{1}{200}$ in all three cases). The three sets of data are found to collapse to the same curve, thereby establishing the validity of the scaling form of Eq. (6). The L dependence of the results shown in Fig. 1 may, therefore, be thought of as representing the dependence of the scaling function f_d on the value of its second argument, $\delta x/L$.

Numerical results for the FIC survival probability Q_{FIC} were reported in Ref. [11] where it was shown that it exhibits the following scaling behavior:

$$Q_{FIC}(x,L,\delta x,w) = f_{FIC}(x/L, \delta x/L, w/W(L)). \tag{7}$$

For the sake of completeness, we have shown in Fig. 4 our numerical results for Q_{FIC} obtained for $w/W(L)=0.02$. Two sets of data are shown, one for $L=800$, obtained from steady-state interfaces generated by numerical integration, and the other for $L=10^4$, obtained from interfaces generated using Gaussian random variables, as outlined above. In both cases, the initial decay of Q_{FIC} can be well represented by a power law, $Q_{FIC}(x) \propto x^{-\theta_{FIC}}$ with $\theta_{FIC}=0.5$. As in the case of the steady-state survival probability, the dependence of Q_{FIC} on the value of L may be thought of as representing the dependence of the scaling function f_{FIC} of Eq. (7) on the argument $\delta x/L$.

III. ANALYTIC CALCULATIONS

In this section, we describe in detail our analytic calculation of the spatial survival probabilities in the stationary state of the 1D EW equation (1). We consider periodic boundary condition, $h(0,t)=h(L,t)$. The height can then be decomposed into a Fourier series, $h(x,t)=\Sigma_k \tilde{h}(k,t)e^{ikx}$ where $k=2\pi m/L$ with $m=0,\pm 1,\pm 2\ldots$. Substituting this in Eq. (1) one finds that different nonzero Fourier modes decouple from each other. This enables an exact calculation of any two-point correlation function. For example, as shown in the Appendix, one finds for any $k\neq 0$, $\langle \tilde{h}(k,t)\tilde{h}(k',t)\rangle = [D'/\Gamma L k^2]\delta_{k+k',0}$ in the stationary limit $t\to\infty$. Note that the $k=0$ mode is identically zero at all times, $\tilde{h}(0,t)=0$, which follows from the sum rule $\int_0^L h(x,t)dx=0$ as the height $h(x,t)$, by definition, is always measured with respect to its spatial average. Since Eq. (1) is linear, the height field $h(x,t)$ is Gaussian for all x and all t. Using the result for the two-point correlator mentioned above, one can then easily write down the joint probability distribution of the Fourier modes in the stationary state,

$$P\{[\tilde{h}(k)]\} \propto \exp\left(-\frac{\Gamma L}{2D'}\sum_k k^2 \tilde{h}(k)\tilde{h}(-k)\right)\delta[\tilde{h}(0)], \quad (8)$$

where the delta function on the right-hand side of Eq. (8) takes care of the "zero-area" constraint. In terms of the actual height field $h(x,t)$, the stationary joint distribution becomes [18,19]

$$P_{\rm st}\{[h(x)]\} = 2\sqrt{\pi D}L^{3/2}\exp\left[-\frac{1}{4D}\int_0^L dx\left(\frac{dh}{dx}\right)^2\right] \times \delta[h(0)-h(L)]\delta\left(\int_0^L h(x)dx\right), \quad (9)$$

where $D=D'/2\Gamma$ and the normalization constant $2\sqrt{\pi D}L^{3/2}$, ensuring that the joint distribution is normalized, can be calculated explicitly [19]. The two delta functions in Eq. (9) respectively take care of the periodic boundary condition $h(0)=h(L)$ and the zero-area constraint. The stationary height distribution at any fixed point x in space is, by translational invariance, independent of x and is also a Gaussian

$$P{\rm st}(h) = \frac{1}{\sqrt{2\pi\langle h^2\rangle}}\exp[-h^2/2\langle h^2\rangle], \quad (10)$$

where the variance $\langle h^2\rangle = D'L/12\Gamma = DL/6$ can be easily computed (see the Appendix).

Note that in the standard literature on interfaces, one often ignores the "zero-area" constraint in the stationary measure [20]. This is justified if one is interested in calculating physical properties in an infinite ($L\to\infty$) system where the zero mode $\tilde{h}(k=0)$ does not play any important role. Besides, in the calculation of certain observables even in a finite system, such as the average width in the stationary state or the distribution of the square of the spatially averaged width [21], the $k=0$ mode drops out of the calculation. However, as pointed out in Refs. [18,19], the zero-area constraint certainly plays a very crucial role in the calculation of, for example, the distribution of the maximal height of the interfaces in a finite system. We will see below that the zero-area constraint does indeed play an important role also in the calculation of spatial survival probabilities in a finite system.

From the expression of the stationary measure in Eq. (9) it is evident that stationary paths are locally Brownian, i.e., evolve in space as, $dh(x)/dx=\xi(x)$, where $\xi(x)$ is a Gaussian white noise with zero mean and a correlator, $\langle \xi(x)\xi(x')\rangle = 2D\delta(x-x')$. For the periodic boundary condition, the stationary path in space is, in fact, a Brownian bridge over $x\in[0,L]$ that starts at $h_0=h(0)$ at $x=0$ and ends up at the same point $h(L)=h_0$ at $x=L$. In addition, this Brownian bridge has a total zero area under it. It turns out to be convenient to perform the calculations using the standard notations of a "temporal" Brownian motion, $dx/dt=\xi(t)$ with $\langle \xi(t)\rangle=0$ and $\langle \xi(t)\xi(t')\rangle = 2D\delta(t-t')$. At the end of the calculations, one can translate back the results to the interface problem upon identifying (*i*) the height of the interface with the position of the temporal Brownian motion, i.e., $h\equiv x$, and (*ii*) the space in the interface problem with the time in the temporal Brownian motion, i.e., $x\equiv t$. Thus, in this notation, the temporal Brownian bridge starts at the initial position x_0 ($\equiv h_0$) at $t=0$ and ends at the same position x_0 after a time interval $t=T$ ($T\equiv L$), and enclosing under it a total zero area, i.e., $\int_0^T x(t)dt=0$.

With these notations set up, we first describe a calculation of the spatial survival probability in which the zero-area constraint is not taken into account. Although the survival probability can be calculated exactly in this case, the resulting analytic expression does not show good agreement with numerical results, implying that the zero-area constraint is crucial for a correct description of the first-passage properties. We then show that the zero-area constraint can be taken into account in a formally exact path integral treatment. This treatment, however, does not lead to a simple closed-form expression for the survival probability that can be compared with numerical results. We then use a "deterministic" approximation to obtain closed-form expressions for the survival probabilities and show that the analytic results obtained this way provide a reasonably good account of the numerical results. Note that since the stationary measure of the 1D KPZ interface for the periodic boundary condition is the same as that in the EW interface [20], all our steady state results will be valid for the 1D KPZ interface as well.

A. Survival probability without the zero-area constraint

Let us first recall some basic results for the ordinary free temporal Brownian motion. Consider a Brownian motion,

$$\frac{dx}{dt} = \xi(t), \quad (11)$$

where $\xi(t)$ is a zero mean Gaussian white noise with correlator $\langle \xi(t)\xi(t')\rangle = 2D\delta(t-t')$. The free propagator of the Brownian motion $G(x,t|x_0,t_0)$ defined as the probability that the particle will reach x at time t starting from x_0 at t_0 can be easily obtained by solving the Fokker-Planck equation,

$$\partial_t G(x,t|x_0,t_0) = D\partial_x^2 G(x,t|x_0,t_0), \tag{12}$$

subject to the initial condition $G(x,t_0|x_0,t_0)=\delta(x-x_0)$ and the boundary conditions that $G\to 0$ as $x\to\pm\infty$. The well known solution is given by

$$G(x,t|x_0,t_0) = \frac{1}{\sqrt{4\pi D(t-t_0)}} \exp[-(x-x_0)^2/4D(t-t_0)], \tag{13}$$

valid for all t and t_0 and x and x_0. We now ask: what is the probability that the particle reaches x at time t, starting at x_0 at t_0, but without having crossed the zero in between? This probability $P(x,t|x_0,t_0)$ can be easily calculated by solving the same Fokker-Planck equation, but now adding an absorbing boundary condition at $x=0$, i.e., insisting that $P(0,t|x_0,t_0)=0$ for all t [22]. The solution can be easily obtained by the image method and is given by

$$P(x,t|x_0,t_0) = \frac{1}{\sqrt{4\pi D(t-t_0)}}\{\exp[-(x-x_0)^2/4D(t-t_0)] - \exp[-(x+x_0)^2/4D(t-t_0)]\}. \tag{14}$$

Evidently, this solution satisfies the absorbing boundary condition at $x=0$.

Now, let us consider a Brownian bridge over the interval $[0,T]$. This means a Brownian motion that starts at x_0 at $t=0$ and ends up at the same point x_0 at time T. Let us ask: what is the probability $Q(t,T|x_0)$ that this process (conditioned to be at x_0 at the two endpoints) does not cross zero in the interval $[0,t]$ where $0\leqslant t\leqslant T$? To calculate this probability, let us divide a typical path of the process over two intervals: $[0,t]$ and $[t,T]$. Over the first interval $[0,t]$, a typical path starts at x_0 at the left end of the interval and lands up, say, at x (where x is a variable) at t, without having crossed the zero over the interval $[0,t]$. This probability for the left interval is [using Eq. (14)]

$$P_L(x,t|x_0,0) = \frac{1}{\sqrt{4\pi Dt}}\{\exp[-(x-x_0)^2/4Dt] - \exp[-(x+x_0)^2/4Dt]\}. \tag{15}$$

Over the second interval $[t,T]$, the path starting at x at t (left end of the interval $[t,T]$) reaches at x_0 at T, but there is no restriction over this second interval (the path is allowed to cross zero in this second interval). Thus, this probability for the right interval is obtained from the free propagator in Eq. (13),

$$P_R(x_0,T|x,t) = \frac{1}{\sqrt{4\pi D(T-t)}} \exp[-(x_0-x)^2/4D(T-t)]. \tag{16}$$

Due to the Markovian property of the walk, the left and right intervals are independent. Hence the net probability is just the product of the two probabilities, integrated over the position x at the intermediate point t over $x\in[0,\infty]$. This will be the total probability that a path starting at x_0 at $t=0$ will end up at x_0 at time T, without having crossed the zero in the interval $[0,t]$. To get the conditional probability $Q(t,T|x_0)$ (conditioned that the two ends are already given to be at x_0), we need to divide this probability by the factor $1/\sqrt{4\pi DT}$ which is just the probability of a free path landing up at x_0 at T, starting at x_0 at time 0. Thus, finally, we get

$$Q(t,T|x_0) = \sqrt{\frac{T}{4\pi Dt(T-t)}}\int_0^\infty dx\{\exp[-(x-x_0)^2/4Dt] - \exp[-(x+x_0)^2/4Dt]\} \times\exp[-(x_0-x)^2/4D(T-t)]. \tag{17}$$

This integral can be done in closed form and one gets

$$Q(t,T|x_0) = \frac{1}{2}\left[1+\mathrm{erf}\left(x_0\sqrt{\frac{T}{4Dt(T-t)}}\right) - \exp(-x_0^2/DT)\mathrm{erfc}\left(x_0\frac{(T-2t)}{\sqrt{4DtT(T-t)}}\right)\right], \tag{18}$$

where $\mathrm{erf}(x)=(2/\sqrt{\pi})\int_0^x e^{-u^2}du$ is the error function and $\mathrm{erfc}(x)=1-\mathrm{erf}(x)$.

So, now we can interpret these results in terms of the stationary state of the EW interfaces. Identifying $x_0\equiv h_0$ and $T\equiv L$ and $t\equiv x$, $Q(x,L|h_0)$ in Eq. (18) is just the probability that the stationary interface, given its height h_0 at the two ends of the sample, does not cross zero in the spatial interval $[0,x]$ and is given by, for $h_0>0$,

$$Q(x,L|h_0) = \frac{1}{2}\left[1+\mathrm{erf}\left(h_0\sqrt{\frac{L}{4Dx(L-x)}}\right) - \exp(-h_0^2/DL)\mathrm{erfc}\left(h_0\frac{(L-2x)}{\sqrt{4DxL(L-x)}}\right)\right]. \tag{19}$$

Now, we need to average $Q(x,L|h_0)$ over the stationary distributions of h_0 given in Eq. (10),

$$Q(x,L) = 2\int_0^\infty dh_0 Q(x,L|h_0)P_{\mathrm{st}}(h_0). \tag{20}$$

The factor 2 comes from the fact that the stationary distribution becomes twice its value if restricted over only the positive half-space $h_0\in[0,\infty]$. The integral in Eq. (20) can be done in closed form. We need to use the identity,

$$\int_0^\infty dx e^{-x^2}\,\mathrm{erf}(zx) = \frac{1}{\pi}\tan^{-1}(z), \tag{21}$$

which can be easily proved by differentiating both sides with respect to z, performing the resulting integral, and then integrating back with respect to z. Our final result is $Q(x,L)=f(x/L)$ for all x and L, where the scaling function $f(u)$ is given exactly by

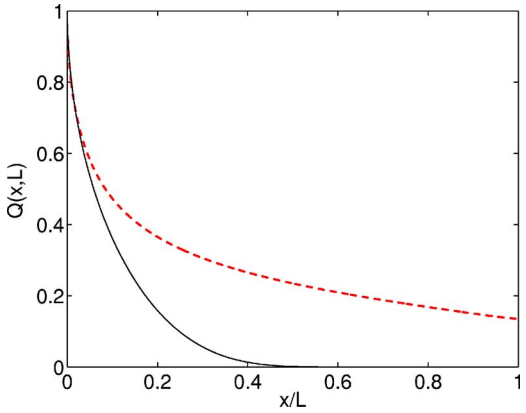

FIG. 5. (Color online) Comparison of the analytic result for the spatial survival probability [Eq. (22) with $u=x/L$, $Q(x,L)=f(u)$], obtained without enforcing the zero-area constraint [(red) dashed line] with the numerical result for $L=10^4$ [(black) solid line].

$$f(u) = \frac{1}{2}\left(1 - \frac{\sqrt{3}}{2}\right) + \frac{1}{\pi}\tan^{-1}\left[\frac{1}{2\sqrt{3}}\frac{1}{\sqrt{u(1-u)}}\right] + \frac{\sqrt{3}}{2\pi}\tan^{-1}\left[\frac{1}{4}\frac{(1-2u)}{\sqrt{u(1-u)}}\right]. \tag{22}$$

One can easily check that $f(0)=1$ as it should be. Also, note that $f(1)=1-\sqrt{3}/2$ is nonzero. Interestingly, this scaling function $f(u)$ does not depend on the system parameters D' or Γ.

The function $f(u)$ in Eq. (22) is plotted versus u in Fig. 5 and compared with the numerical result obtained for $L=10^4$. The agreement between the analytic and numerical results is not satisfactory. In particular, the numerical result for $f(u)$ goes to very small values as u is increased above 0.5, while the analytic curve shows a finite value $f(1)=1-\sqrt{3}/2$ even at $u=1$. It is, therefore, clear that the zero-area constraint has to be included in the calculation for a correct description of the survival probability.

B. Survival probability with the zero-area constraint

In the previous section, we did not take into account the constraint that the total area under the Brownian bridge $x(\tau)$ going from x_0 at time $\tau=0$ to x_0 at time $\tau=T$ is actually zero. In this subsection, we perform the calculation taking into account this zero-area constraint.

We first define $Q_0(t,T|x_0)$ to be the probability that the process $x(\tau)$ starting at x_0 at $\tau=0$ does not cross zero up to time t (see Fig. 6) where $0\leqslant t\leqslant T$, *given that the process ends up at* x_0 *at* $\tau=T$ *and that the total area under the process from* 0 *to* T *is* 0. The subscript 0 in Q_0 indicates the fact that we are considering only those paths (out of all possible paths starting at x_0) whose area is 0. Note that the analogous quantity $Q(t,T|x_0)$ without the area constraint was computed in Eq. (18). Formally, one can express this probability $Q_0(t,T|x_0)$ as follows,

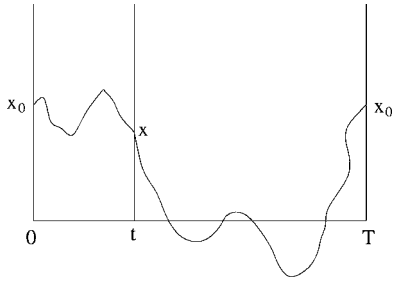

FIG. 6. A typical Brownian path starting at x_0 and reaching x at time t without crossing the origin and then freely propagating from x at t to x_0 at time T.

$$Q_0(t,T|x_0) = \frac{\left\langle \left[\prod_{\tau=0}^{t}\theta(x(\tau))\right]\delta[x(T)-x_0]\delta\left[\int_0^T x(\tau)d\tau\right]\right\rangle}{\left\langle \delta[x(T)-x_0]\delta\left[\int_0^T x(\tau)d\tau\right]\right\rangle}, \tag{23}$$

where the angular brackets $<\cdots>$ denote an average over all possible Brownian paths that start at x_0 at time 0. The numerator $\mathcal{N}$ in Eq. (23) represents the joint probability of three events: (*i*) the probability that the path does not cross zero up to t (the first factor), (*ii*) the probability that the path finally ends up at x_0 at time $\tau=T$ (the second factor), and (*iii*) the probability that the area under the process upto time T is zero (the third factor). The denominator $\mathcal{D}$ in Eq. (23) represents the joint probability of events (*ii*) and (*iii*). So, the ratio $\mathcal{N}/\mathcal{D}$ represents the conditional probability $Q_0(t,T|x_0)$, i.e., the fraction of paths that start at x_0 and satisfy (*i*), (*ii*), and (*iii*), out of all paths that start at x_0 and satisfy (*ii*) and (*iii*).

This numerator can further be split into two parts: (a) the probability that a path starting at x_0 reaches x at the intermediate time t without crossing zero and enclosing an area, say $A>0$ (the area is positive since the path does not cross zero in $[0,t]$), and (b) the subsequent probability that the path starting at x at time t reaches x_0 at time T and enclosing an area $-A$. This ensures that the total area up to T is zero. However, we then have to integrate over all possible values of $A>0$ and $x>0$. Thus, one can rewrite Eq. (23) as

$$Q_0(t,T|x_0) = \frac{\int_0^\infty dA\int_0^\infty dx G^+(x,A,t|x_0,0,0)G(x_0,-A,T-t|x,0,0)}{G(x_0,0,T|x_0,0,0)}, \tag{24}$$

where we define $G(x,A,t|x_0,A_0,0)$ to be the probability that the joint two-variable Gaussian process $[x(t),A(t)=A_0+\int_0^t x(\tau)d\tau]$ (i.e., the Brownian curve itself and the integral under the Brownian curve) reaches $[x,A]$ at time t, starting from the initial value $[x_0,A_0]$ at time 0. So, $G(x,A,t|x_0,A_0,0)$ is just the propagator for this joint Gauss-

ian process. Note that this process is free in the sense that it has no restriction for $x(t)$ to be only positive. Clearly, the denominator $\mathcal{D}$ in Eq. (23) is just $G(x_0,0,T|x_0,0,0)$ since, by definition, this quantity represents the probability the process $[x(t),A(t)]$ will reach its final value $[x_0,0]$ (note that the final area is zero) at time T, starting from its initial value $[x_0,0]$ (since the initial area is zero). Similarly, the part (b) in the numerator is just $G(x_0,-A,T-t|x,0,0)$ since that represents the joint probability that a path starting at x at time t and initial area 0 will end at x_0 at time T with area $-A$ (note that we have made a shift $[t,T]\to[0,T-t]$ which is allowed due to time translational invariance of Brownian motion). Finally we define $G^+(x,A,t|x_0,0,0)$ to be the joint probability that the process $[x(t),A(t)]$ will reach $[x,A]$ at time t starting from $[x_0,0]$ and *without* x crossing the origin in the interval $[0,t]$.

Now, the free propagator $G(x,A,t|x_0,A_0,0)$ is easy to compute. This is just the joint bivariate Gaussian distribution of the random variable $x(t)$ and $A(t)=A_0+\int_0^t x(t')dt'$. Their correlation matrix can be easily computed and the propagator is just the exponential of the inverse correlator. Indeed, this result is already well known, since this is just a random acceleration problem: $dA/dt=x(t)$ and $dx/dt=\eta(t)$ which implies $d^2A/dt^2=\eta(t)$. The result for the propagator can be found, for example, in Refs. [19,23]. We just quote this result here,

$$G(x,A,t|x_0,A_0,0)=\frac{\sqrt{3}}{2\pi Dt^2}\exp\left[-\frac{1}{D}\left(\frac{3}{t^3}(A-A_0-xt)\times(A-A_0-x_0t)+\frac{1}{t}(x-x_0)^2\right)\right]. \quad (25)$$

Substituting this exact propagator in Eq. (24), we get

$$Q_0(t,T|x_0)=\left(\frac{T}{T-t}\right)^2\exp(3x_0^2/DT)\times\int_0^\infty dA\int_0^\infty dx G^+(x,A,t|x_0,0,0)\times\exp\left[-\frac{3}{D(T-t)^3}[A+x(T-t)][A+x_0(T-t)]-\frac{1}{D(T-t)}(x-x_0)^2\right]. \quad (26)$$

Note that we still have to determine the restricted propagator $G^+(x,A,t|x_0,0,0)$ and then we have to average $Q(t,T|x_0)$ over the stationary distribution of x_0 to calculate $Q_0(t,T)=2\int_0^\infty dx_0 Q_0(t,T,x_0)P_{\rm st}(x_0)$, where the distribution $P_{\rm st}(x_0)$ is given in Eq. (10). With the identification $h_0\equiv x_0$ and $L\equiv T$, one gets

$$P_{\rm st}(x_0)=\sqrt{\frac{3}{\pi DT}}\exp(-3x_0^2/DT), \quad (27)$$

which gives

$$Q_0(t,T)=2\sqrt{\frac{3}{\pi DT}}\int_0^\infty dx_0 e^{-3x_0^2/DT}Q_0(t,T,x_0). \quad (28)$$

Substituting the expression of $Q_0(t,T|x_0)$ from Eq. (26) in Eq. (28), we find that the factor $\exp(-3x_0^2/DT)$ cancels out and we get a formally exact result,

$$Q_0(t,T)=4\sqrt{3}\sqrt{\frac{t}{T}}\left(\frac{T}{T-t}\right)^2\int_0^\infty\frac{dx_0}{\sqrt{4\pi Dt}}\times\int_0^\infty dx\int_0^\infty dA G^+(x,A,t|x_0,0,0)\times\exp\left(-\frac{3}{D(T-t)^3}[A+x(T-t)][A+x_0(T-t)]-\frac{1}{D(T-t)}(x-x_0)^2\right). \quad (29)$$

So the remaining task is to evaluate the restricted propagator $G^+(x,A,t|x_0,0,0)$ which we do in the next two subsections.

1. Exact calculation of the restricted propagator G^+

We note that the restricted propagator $G^+(x,A,t|x_0,0,0)$ is just the joint probability that the process $x(t)$ starting at x_0 at time 0 reaches x at time t without crossing the origin and that the area under the curve is A. Thus it is given by

$$G^+(x,A,t|x_0,0,0)=\left\langle\left(\prod_{\tau=0}^{t}\theta(x(\tau))\right)\delta[x(t)-x]\delta\left(\int_0^t x(\tau)d\tau-A\right)\right\rangle, \quad (30)$$

where the angular brackets $\langle\cdots\rangle$ denote an average over all possible paths starting at x_0 at time 0. Note that if $x_0=x=0$, this restricted Brownian process is just a Brownian excursion over the interval $[0,t]$ and the propagator $G^+(0,A,t|0,0,0)$ is just the (unnormalized) probability density of the area under a Brownian excursion. A Brownian excursion is simply a Brownian path that propagates from $x(0)=0$ to $x(t)=0$ over $[0,t]$ but is conditioned to stay positive in between. The probability distribution of the area under a Brownian excursion was calculated exactly and is known as the Airy distribution function, a complicated function that involves the zeros of the Airy function but is not the Airy function itself [24–28]. This Airy distribution function has been a subject of intense study for the past several years as it has resurfaced in many problems in computer science [26,27], graph theory [29], and two-dimensional polygon problems [30]. Recently it was shown that the same Airy distribution function also describes the distribution of maximal height in the stationary state of fluctuating interfaces [18,19]. In Ref. [19], a path integral derivation of the area distribution under a Brownian excursion was provided. In our present problem, we have a generalization of this problem where a Brownian path propagates from x_0 at $\tau=0$ to x at $\tau=t$, staying positive in between. The nonzero values of the initial and the final positions, x_0 and x, make explicit calculation of the distribution of the area

under such a path difficult, as demonstrated below. Here we follow the path integral method used in Ref. [19] generalized to nonzero x_0 and x.

Let us define the Laplace transform of G^+ with respect to the area A, i.e.,

$$\tilde{G}(x,x_0,t,\lambda) = \int_0^\infty G^+(x,A,t|x_0,0,0)e^{-\lambda A}dA. \tag{31}$$

Note that since the path is restricted to be on the positive side, the area is always positive and hence a Laplace transform (rather than a Fourier transform) is more suitable. Taking Laplace transform of Eq. (30) we get

$$\tilde{G}(x,x_0,t,\lambda) = \left\langle \left(\prod_{\tau=0}^{t} \theta(x(\tau)) \right) \delta[x(t)-x] \times \exp\left[-\lambda \int_0^t x(\tau)d\tau \right] \right\rangle. \tag{32}$$

Using the Brownian measure of the paths in Eq. (9), $\tilde{G}(x,x_0,t,\lambda)$ can be expressed as a path integral,

$$\tilde{G}(x,x_0,t,\lambda) \propto \int_{x(0)=x_0}^{x(t)=x} \mathcal{D}x(\tau)\theta[x(\tau)] \times \exp\left\{ -\int_0^t d\tau \left[\frac{1}{4D}\left(\frac{dx(\tau)}{d\tau} \right)^2 + \lambda x(\tau) \right] \right\}. \tag{33}$$

Using the bra-ket notation, one can reexpress the right-hand side of Eq. (33) as a quantum mechanical propagator,

$$\tilde{G}(x,x_0,t,\lambda) = \langle x_0|e^{-\hat{H}t}|x\rangle, \tag{34}$$

where the Hamiltonian $\hat{H}$ can be written (in the position basis)

$$\hat{H} = -D\frac{d^2}{dx^2} + V(x), \tag{35}$$

where the quantum potential $V(x)=\lambda x$ for $x>0$ and in addition $V(0)=\infty$ (i.e., there is a hard wall at the origin) which takes into account the fact that all paths in Eq. (33) are restricted to be on the positive side and cannot enter the region $x<0$. Expanding the right-hand side of Eq. (34) in the eigenbasis of the Hamiltonian $\hat{H}$ we get

$$\tilde{G}(x,x_0,t,\lambda) = \sum_E \langle x_0|E\rangle\langle E|x\rangle e^{-Et} = \sum_E \psi_E(x)\psi_E^*(x_0)e^{-Et}, \tag{36}$$

where E denotes the eigenvalues of $\hat{H}$ and the eigenfunction $\psi_E(x)$ satisfies the Schrodinger equation in the region $x \in [0,\infty]$,

$$-D\frac{d^2}{dx^2}\psi(x) + \lambda x\psi(x) = E\psi(x), \tag{37}$$

with the boundary conditions $\psi(\infty)=0$ and $\psi(0)=0$, the latter reflecting the hard wall at the origin. Making the change of variable, $z=(\lambda/D)^{1/3}(x-E/\lambda)$, one can recast the Schrodinger equation as the following Airy differential equation,

$$\frac{d^2\psi}{dz^2} - z\psi = 0, \tag{38}$$

whose general solution is given in terms of two Airy functions,

$$\psi(z) = B\,\mathrm{Ai}(z) + C\,\mathrm{Bi}(z), \tag{39}$$

where B and C are arbitrary constants. The function $\mathrm{Bi}(z)$ diverges as $z\to\infty$ (see Ref. [31]) indicating $C=0$. Going back to the original x variable, we have

$$\psi(x) = B\,\mathrm{Ai}\left[\left(\frac{\lambda}{D} \right)^{1/3} \left(x - \frac{E}{\lambda} \right) \right]. \tag{40}$$

The other boundary condition $\psi(x=0)=0$ determines the eigenvalues,

$$\mathrm{Ai}\left[-\frac{E}{(D\lambda^2)^{1/3}} \right] = 0. \tag{41}$$

It is known (see Ref. [31], p. 446) that the Airy function $\mathrm{Ai}(x)$ has zeroes on the negative x axis at $x=-\alpha_i$. For example, $\alpha_1=2.33$, $\alpha_2=4.08$, $\alpha_3=5.52$, $\alpha_4=6.78$, etc. Thus we get the exact eigenvalues

$$E_i = \alpha_i(D\lambda^2)^{1/3}. \tag{42}$$

The amplitude B in Eq. (40) is determined from the normalization, $\int_0^\infty |\psi_E(x)|^2dx=1$ and we get

$$|B_i|^2 = \frac{1}{\int_0^\infty \mathrm{Ai}^2[(\lambda/D)^{1/3}y - \alpha_i]dy}. \tag{43}$$

Finally, putting everything back in Eq. (36) we get the exact Laplace transform of the restricted propagator,

$$\tilde{G}(x,x_0,t,\lambda) = \sum_{\alpha_i} \frac{\mathrm{Ai}[(\lambda/D)^{1/3}x_0 - \alpha_i]\mathrm{Ai}[(\lambda/D)^{1/3}x - \alpha_i]}{\int_0^\infty \mathrm{Ai}^2[(\lambda/D)^{1/3}y - \alpha_i]dy} \times \exp(-\alpha_i D^{1/3}\lambda^{2/3}t), \tag{44}$$

where $-\alpha_i$'s are the zeros of the Airy function $\mathrm{Ai}(x)$. Formally inverting the Laplace transform using the Bromwitch formula, we get the exact expression for the restricted propagator,

$$G^+(x,A,t|x_0,0,0) = \int_{\lambda_0-i\infty}^{\lambda_0+i\infty} \frac{d\lambda}{2\pi i} e^{\lambda A}\tilde{G}(x,x_0,t,\lambda), \tag{45}$$

where $\tilde{G}(x,x_0,t,\lambda)$ is given by Eq. (44) and the integration is along any imaginary axis whose real part λ_0 must be to the right of all singularities of the integrand.

Substituting this restricted propagator from Eqs. (45) and (44) in Eq. (29) gives us the formal exact answer of the no zero crossing probability $Q_0(t,T)$ which, one can easily check, has the scaling form $Q_0(t,T)=f(t/T)$. However, this formal expression of the scaling function $f(u)$, though exact,

is hardly useful to make comparison with the numerical data. This is because we cannot invert the Laplace transform explicitly in Eq. (45). [Even after that one needs to do the three integrals over x_0, x, and A in Eq. (29), which looks hopeless!]

So, the question is: Can one find an approximate way to estimate the restricted propagator $G^+(x,A,t|x_0,0,0)$ and then use this approximate result in Eq. (29), do the three integrals, and derive an explicit expression for the scaling function $f(u)$? In the next subsection, we indeed perform these steps and derive an explicit expression of $f(u)$ which, though not exact, is expected to be quite good.

2. A deterministic approximation for the restricted propagator G^+

As a first step, let us rewrite the restricted propagator $G^+(x,A,t|x_0,0,0)$ in Eq. (30) as follows,

$$\begin{aligned} G^+(x,A,t|x_0,0,0) &= \left(\frac{\langle [\prod_{\tau=0}^{t} \theta(x(\tau))]\delta[x(t)-x]\delta[\int_0^t x(\tau)d\tau - A]\rangle}{\langle [\prod_{\tau=0}^{t} \theta(x(\tau))]\delta[x(t)-x]\rangle} \right) \\ &\times \left\langle \left(\prod_{\tau=0}^{t} \theta(x(\tau)) \right) \delta[x(t)-x] \right\rangle \\ &= W[A,x,x_0,t]P(x,t|x_0,0), \end{aligned} \tag{46}$$

where we just divided and multiplied the right-hand side of Eq. (30) by the same factor $P(x,t|x_0,0) = \langle [\Pi_{\tau=0}^{t} \theta(x(\tau))]\delta[x(t)-x]\rangle$. This factor is simply the probability that the path starting at x_0 at time 0 reaches x at time t without crossing the origin in the interval $[0,t]$ and has already been calculated by the image method in Eq. (14). Thus, we have

$$\begin{aligned} P(x,t|x_0,0) &= \left\langle \left(\prod_{\tau=0}^{t} \theta(x(\tau)) \right) \delta[x(t)-x] \right\rangle \\ &= \frac{1}{\sqrt{4\pi D t}} \{ \exp[-(x-x_0)^2/4Dt] \\ &\quad - \exp[-(x+x_0)^2/4Dt] \}. \end{aligned} \tag{47}$$

The quantity $W(A,x,x_0,t)$ represents the expression inside the first parenthesis on the right-hand side of Eq. (46) which we can write as

$$W(A,x,x_0,t) = \frac{\langle \delta[\int_0^t x(\tau)d\tau - A][\prod_{\tau=0}^{t} \theta(x(\tau))]\delta[x(t)-x]\rangle}{\langle [\prod_{\tau=0}^{t} \theta(x(\tau))]\delta[x(t)-x]\rangle}, \tag{48}$$

which is simply the probability distribution of the the area under the process in $[0,t]$, *given that the process reaches from x_0 to x in time t without crossing the origin in between*.

So, if we can estimate this conditional area distribution $W(A,x,x_0,t)$, then, knowing the exact $P(x,t|x_0,0)$ from Eq. (47), we will be able to estimate the restricted propagator $G^+(x,A,t|x_0,0,0)$ from Eq. (46).

Note that so far we have not made any approximation. To estimate the conditional area distribution $W(A,x,x_0,t)$ defined in Eq. (48), we now make a "deterministic" approximation as follows. Note that $W(A,x,x_0,t)$ is just the fraction of paths that have an area A, amongst all possible paths that go from x_0 to x without crossing the origin in between. Now, the paths that go from x_0 at $\tau=0$ to x at $\tau=t$ without crossing the origin in between are likely to cluster around an *optimal* path, i.e., most of these paths lie "close" to an optimal path. This optimal path is the one which has the highest probability amongst all possible paths going from x_0 at $\tau=0$ to x at $\tau=t$ without crossing the origin in between. Assuming the existence of such an optimal path $x_{\rm opt}(\tau)$, the "deterministic" approximation consists in writing

$$W(A,x_0,x,t) \approx \delta\left(A - \int_0^t x_{\rm opt}(\tau)d\tau \right). \tag{49}$$

Thus, within this aproximation we ignore the fluctuations that arise from nonoptimal paths.

The next step is to actually find the optimal path $x_{\rm opt}(\tau)$, i.e., the path with the highest probability, amongst all possible paths that satisfy the following constraints: (*i*) $x(0)=x_0$, (*ii*) $x(t)=x$, and (*iii*) $x(\tau)>0$ for all $0\leqslant\tau\leqslant t$, i.e., the path stays positive in the interval $\tau\in[0,t]$. One knows from the principle of least actions that the optimal path is the so-called "classical" path that satisfies Newton's equation of motion. In our problem, the action in the path integral, $S=(1/4D)\int_0^t [dx(\tau)/d\tau]^2 d\tau$, corresponds to that of a free particle. So, the optimal path satisfies the Newton's law for a free partricle, namely $d^2x/d\tau^2=0$, starting from $x(0)=x_0$ and ending at $x(t)=x$ for all $0\leqslant\tau\leqslant t$. The solution is trivially,

$$x_{\rm opt}(\tau) = x_0 + (x-x_0)\frac{\tau}{t}. \tag{50}$$

Note that this solution automatically satisfies the condition (*iii*) mentioned above, i.e., it stays positive in the interval $\tau\in[0,t]$. Now, the area under the optimal path is simply

$$A_{\rm opt} = \int_0^t x_{\rm opt}(\tau)d\tau = \frac{1}{2}(x_0+x)t. \tag{51}$$

Before proceeding to the calculation of the survival probability with this optimal choice, it is instructive to ask how the calculated survival probability depends on the choice of the deterministic path. In other words, within the deterministic approximation in Eq. (49), how does the final result vary if instead of the optimal path in Eq. (50), we use some other paths? To test this, we actually consider a one-parameter family of paths that satisfy the constraints (*i*), (*ii*), and (*iii*) above. This family of paths is characterized by a single parameter $\beta>0$,

$$x_\beta(\tau) = x_0 + (x-x_0)\left(\frac{\tau}{t}\right)^\beta. \tag{52}$$

Clearly, as shown above, $\beta=1$ corresponds to the optimal path. In the following, we will however calculate the survival

probability for all $\beta>0$ to test how sensitive the final answer is to the optimal choice $\beta=1$. We will see, somewhat surprisingly, that the final scaling function $f(u)$ characterising the survival probability depends only very weakly on β.

The area under the deterministic path in Eq. (52) is simply

$$A(\beta,x_0,x,t)=\int_0^t x_\beta(\tau)d\tau=[ax_0+(1-a)x]t, \quad \text{where } a=\frac{\beta}{1+\beta}. \tag{53}$$

The optimal path corresponds to the choice $\beta=1$, i.e., $a=\frac{1}{2}$. Our approximation in Eq. (49) then reads

$$W(A,x,x_0,t)\approx\delta(A-[ax_0+(1-a)x]t), \tag{54}$$

the optimal choice being $a=\frac{1}{2}$.

Within this deterministic approximation, we then have an explicit expression for the restricted propagator [on substituting the results in Eqs. (47) and (54) in Eq. (46)],

$$G^+(x,A,t|x_0,0,0)\approx\frac{\delta[A-(ax_0+(1-a)x)t]}{\sqrt{4\pi Dt}}\times\{\exp[-(x-x_0)^2/4Dt]-\exp[-(x+x_0)^2/4Dt]\}. \tag{55}$$

3. Explicit expression for the scaling function $f(u)$ using the deterministic approximation

On substituting the expression of $G^+(x,A,t|x_0,0,0)$ from Eq. (55) into Eq. (29), we can do the integral over A trivially, since it involves a delta function. Inside the exponential on the right-hand side of Eq. (29), we have to replace A by $[ax_0+(1-a)x]t$. This gives

$$Q_0(t,T)=4\sqrt{3}\sqrt{\frac{t}{T}}\left(\frac{T}{T-t}\right)^2\int_0^\infty\frac{dx_0}{\sqrt{4\pi Dt}}\int_0^\infty\frac{dx}{\sqrt{4\pi Dt}}\times\{\exp[-(x-x_0)^2/4Dt]-\exp[-(x+x_0)^2/4Dt]\}\times\exp\left(-\frac{3}{D(T-t)^3}[a(x_0-x)t+xT]\times[(1-a)(x-x_0)t+x_0T]-\frac{1}{D(T-t)}(x-x_0)^2\right). \tag{56}$$

We next define the scaling variables: $y=x_0/\sqrt{4Dt}$, $z=x/\sqrt{4Dt}$, and $u=t/T$. Then $Q_0(t,T)$ in Eq. (56) becomes only a function of $u=t/T$, i.e., $Q_0(t,T)=f(t/T)$ where the scaling function $f(u)$ is given from Eq. (56),

$$f(u)=\frac{4\sqrt{3u}}{\pi(1-u)^2}\int_0^\infty dy\int_0^\infty dz[e^{-(y-z)^2}-e^{-(y+z)^2}]\times\exp\left(-\frac{4u}{(1-u)^3}\{[\gamma u^2+(3a-2)u+1]y^2+[\gamma u^2+(1-3a)u+1]z^2+[1+u-2\gamma u^2]yz\}\right), \tag{57}$$

where $\gamma=1-3a+3a^2$. The right hand side of Eq. (57) can be reorganized as,

$$f(u)=\frac{4\sqrt{3u}}{\pi(1-u)^2}[I_1(u)-I_2(u)], \tag{58}$$

where

$$I_1(u)=\int_0^\infty\int_0^\infty dydz\exp[-r(u)y^2-s(u)z^2+p(u)yz],$$

$$I_2(u)=\int_0^\infty\int_0^\infty dydz\exp[-r(u)y^2-s(u)z^2+q(u)yz], \tag{59}$$

where $r(u)=[3(1-4a+4a^2)u^3+(12a-5)u^2+u+1]/(1-u)^3$, $s(u)=[3(1-4a+4a^2)u^3+(7-12a)u^2+u+1]/(1-u)^3$, $p(u)=2[3(1-4a+4a^2)u^3+u^2-5u+1]/(1-u)^3$ and $q(u)=-2[(-5+12a-12a^2)u^3+5u^2-u+1]/(1-u)^3$. To do the double integrals in Eq. (59), it is convenient to scale $y=Y/\sqrt{r(u)}$ and $z=Z/\sqrt{s(u)}$. This gives

$$I_1(u)=\frac{(1-u)^3}{\sqrt{B(u)}}\int_0^\infty\int_0^\infty dYdZ\exp[-(Y^2+Z^2+2A_1(u)YZ)],$$

$$I_2(u)=\frac{(1-u)^3}{\sqrt{B(u)}}\int_0^\infty\int_0^\infty dYdZ\exp[-(Y^2+Z^2+2A_2(u)YZ)], \tag{60}$$

where

$$B(u)=[3(1-4a+4a^2)u^3+(12a-5)u^2+u+1)\times(3(1-4a+4a^2)u^3+(7-12a)u^2+u+1],$$

$$A_1(u)=-\frac{3(1-4a+4a^2)u^3+u^2-5u+1}{\sqrt{B(u)}},$$

$$A_2(u)=\frac{(-5+12a-12a^2)u^3+5u^2-u+1}{\sqrt{B(u)}}. \tag{61}$$

We next use the identity

$$\int_0^\infty\int_0^\infty dYdZ\exp[-(Y^2+Z^2+2AYZ)]=\frac{1}{4}\int_0^\pi\frac{d\theta}{1+A\sin(\theta)}, \tag{62}$$

which can be easily established by going to the polar coordinates $Y=R\cos(\theta)$ and $Z=R\sin(\theta)$ and by performing the

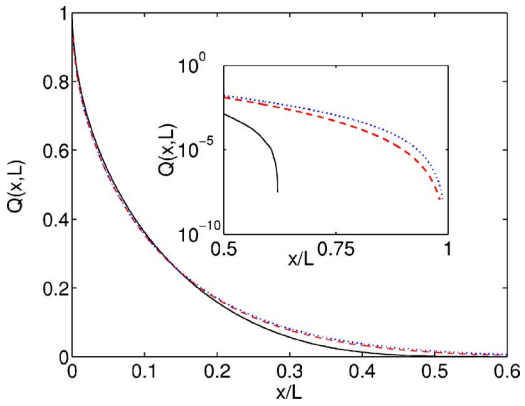

FIG. 7. (Color online) Comparison of the analytic result for the spatial survival probability [Eq. (64) with $u=x/L$, $Q(x,L)=f(u)$], obtained with the zero-area constraint and using the deterministic approximation with $a=\frac{1}{2}$ [(red) dashed line] with the numerical result for $L=10^4$ [(black) solid line]. The analytic result for $f(u)$ obtained using $a=0.1$ is also shown [(blue) dotted line] for comparison. The inset shows the same three plots for larger values of u, using a logarithmic y scale to illustrate the dependence of $f(u)$ on the parameter a for relatively large values of u.

radial integration. The integral $J(A)=\int_0^\pi d\theta/[1+A\sin(\theta)]$ can be done in closed form and one obtains

$$J(A)=\frac{1}{\sqrt{1-A^2}}[\pi-2\sin^{-1}(A)] \quad \text{for } |A|<1,$$

$$=\frac{1}{\sqrt{A^2-1}}\log\left(\frac{A+\sqrt{A^2-1}}{A-\sqrt{A^2-1}}\right) \quad \text{for } |A|>1. \tag{63}$$

Putting all these results back in Eq. (58), we get an explicit result for the scaling function $f(u)$,

$$f(u)=\frac{\sqrt{3}}{\pi}\frac{\sqrt{u}(1-u)}{\sqrt{B(u)}}[J(A_1(u))-J(A_2(u))], \tag{64}$$

where the functions J, A_1, A_2 and B are given respectively in Eqs. (61) and (63). This is our main result, obtained using the deterministic approximation where we keep only the contribution from the optimal path but ignore the fluctuations around the optimal path.

The function in Eq. (64) can be easily evaluated for all $0\leqslant a\leqslant 1$. Note that, by definition, the a dependence of $f(u)$ is symmetric about $a=\frac{1}{2}$, so it suffices to use $0\leqslant a\leqslant\frac{1}{2}$ with $a=\frac{1}{2}$ being the optimal choice. In Fig. 7 we compare the analytically obtained $f(u)$ corresponding to the optimal choice $a=\frac{1}{2}$ with the actual $f(u)$ obtained via numerical simulation on a latice of $L=10^4$ sites. The analytical scaling function $f(u)$ seems to compare well with the numerical one, given especially the fact that there was no fitting parameter involved.

The function $f(u)$ turns out to be rather insensitive to the value of the parameter a. In Fig. 7, we have also plotted $f(u)$ for the choice $a=0.1$. The $f(u)$ obtained for this nonoptimal choice of a is virtually indistinguishable from that obtained for the optimal choice, $a=\frac{1}{2}$. This can be understood from the asymptotic behavior of $f(u)$ near $u=0$. As $u\to 0$, one can show that

$$f(u)=1-\frac{4\sqrt{3u}}{\pi}+\frac{8}{\pi\sqrt{3}}u^{3/2}+\frac{4\sqrt{3}}{\pi}u^{5/2}-\frac{32\sqrt{3}a(1-a)}{\pi}u^{7/2}+O(u^{9/2}). \tag{65}$$

Note that the a dependence appears only in the fifth term in the small-u expansion, showing that the function $f(u)$ is highly insensitive to a for small u. Since $f(u)$ decreases rapidly with increasing u, the dependence of $f(u)$ on a for relatively large values of u is not visible in the linear plot in Fig. 7. This dependence is evident from the plots in the inset of Fig. 7 where the results for $f(u)$ for two different values of a (the optimal value, $a=\frac{1}{2}$, and $a=0.1$) are shown in a logarithmic scale and compared with the numerical data for $L=10^4$.

The dependence of $f(u)$ on the parameter a for relatively large values of u is clearly seen in the asymptotic behavior of $f(u)$ as $u\to 1$. One finds that in powers of $\epsilon=1-u$, where $\epsilon\to 0$,

$$f(u=1-\epsilon)=c_4(a)\epsilon^4+c_5(a)\epsilon^5+c_6(a)\epsilon^6+O(\epsilon^7), \tag{66}$$

where the coefficients $c_4(a)$, $c_5(a)$, $c_6(a)$, etc. are complicated functions of the parameter a. In particular, for the optimal case $a=\frac{1}{2}$, we get

$$f(u=1-\epsilon)=\frac{4}{9\sqrt{3}\pi}\epsilon^4+\frac{2}{3\sqrt{3}\pi}\epsilon^5+\frac{209}{270\sqrt{3}\pi}\epsilon^6+O(\epsilon^7). \tag{67}$$

C. Survival probability for finite initial conditions

Analytic results for the FIC spatial survival probability Q_{FIC} discussed in Sec. I may be obtained from the calculations described above in the following way. We consider the probability that, given the constraint that the height h_0 at $x=0$ lies between $-w$ and $+w$ with $w\ll W(L)$, the steady-state width of the interface of size L, the interface height does not cross zero within distance x. This probability is normalized by the probability of finding the initial height between $-w$ and $+w$ (i.e., by $2\int_0^w P_{st}(h)dh$ where $P_{st}(h)$ is the Gaussian probability distribution for the height in the steady state [see Eq. (3)]). In the first calculation without the zero-area constraint, we use Eq. (19) and integrate the quantity $Q(x,L|h_0)P_{st}(h_0)$ over h_0 between 0 and w (with a factor 2 to take care of negative values), assuming that $w/W(L)\ll 1$, and $u=x/L$ is of order unity. Keeping terms of the lowest (linear) order in $y=w/W(L)$ in the expansions of the exponentials and error functions (the latter is justified as long as u is not very close to 0 or 1), we get the following result for the normalized probability that the height does not cross zero within distance $x=uL$, when the initial height lies between $-w$ and $+w$ with $w=yW(L)$:

$$Q_{FIC}(x,L,w)=\frac{y}{\sqrt{24\pi}}\sqrt{(1-u)/u}. \tag{68}$$

This is clearly consistent with the scaling form of Eq. (7)—the sampling interval δx is zero in the present continuum

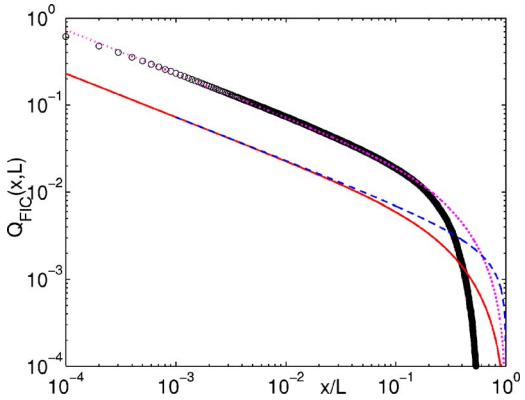

FIG. 8. (Color online) Comparison of analytic and numerical results for the FIC spatial survival probability $Q_{FIC}(x,L,w)$ with $w/W(L)=0.02$. The (blue) dashed line and the (red) solid line show, respectively, the analytic results obtained without the zero-area constraint [Eq. (68)] and with the zero-area constraint [Eq. (69) with $a=\frac{1}{2}$]. The numerical results for $L=10^4$ are shown by (black) circles, and the (magenta) dotted line going through these data points represents the result of Eq. (69) multiplied by 3.167.

description. For small u, the scaling function shows a power-law decay with exponent $\frac{1}{2}$, $f_{FIC}(u,0,y)\sim A(y)/\sqrt{u}$, with $A(y)=y/\sqrt{24\pi}$.

In the calculation with the zero-area constraint, we use the results obtained above using the deterministic approximation. Specifically, we consider Eq. (56) (with t replaced by x and T replaced by L, so that $u=t/T=x/L$) and do the x_0 integration between 0 and w instead of between 0 and ∞, and then divide the result by $[2\int_0^w P_{st}(h)dh]$ for normalization. Again, keeping terms to the lowest order in $y=w/W(L)$, we obtain the result

$$Q_{FIC}(x,L,w)=f_{FIC}(u,0,y)=\sqrt{1/(96\pi)}y\frac{(1-u)[A_2(u)-A_1(u)]r(u)}{\sqrt{uB(u)}}, \tag{69}$$

where the functions $A_1(u)$, $A_2(u)$, and $B(u)$ are defined in Eq. (61) and $r(u)$ is defined in the line after Eq. (59). We use the optimal value, $a=\frac{1}{2}$, in evaluating these functions. In the small-u limit, this expression reduces to the same form, $A(y)/\sqrt{u}$, as that found in the calculation without the zero-area constraint. This is expected, since the zero-area constraint becomes important for values of x comparable to L.

As shown in Fig. 8 where we have plotted the scaling functions according to Eqs. (68) and (69) for $w/W(L)=0.02$ vs. $u=x/L$ on a log-log scale, the results obtained with and without the zero-area constraint agree with each other for small u, but show differences as u increases above about 0.01. In the same figure, we have also shown the numerical results obtained for the same value of y and $L=10^4$. The numerical data show the expected $A/\sqrt{u}$ behavior for small u, but the coefficient A obtained from a fit to the numerical data turns out to be substantially larger than the value $0.02/\sqrt{24\pi}\simeq 0.0023$ predicted by the analytic calculation—the value of A obtained from the fit is close to 0.0073. In Fig. 8, we have also shown the result of Eq. (69) multiplied by 3.167, to take into account this difference between the two values of A. It is clear from the plots that the analytic result multiplied by this empirical factor provides a good description of the numerical data—the level of agreement is roughly similar to that found in Fig. 7 for the steady-state survival probability.

The reason for the necessity of multiplying the analytic result by a numerical factor in order to obtain approximate agreement with the numerical result lies in the use of discrete sampling in the numerical calculation of the FIC survival probability. In Eqs. (68) and (69) above, the survival probability goes to zero as $y\to 0$. This reflects the fact that in the continuum limit, the probability of not crossing zero over a finite distance $x=uL$ is zero if the initial height is zero. This, however, is not true when the sampling of the height is done at discrete points, $x_n=n\delta x$, where n is a positive integer and δx is the sampling interval, taken to be equal to the spatial discretization scale ($\delta x=1$) for most of the numerical results reported here. This is because the probability calculated in the numerical work does not take into account the (many) zero crossings that would have taken place between x_1 and x_2 in the continuum limit if $h(x_1)$ is very close to 0. Even if the height at the initial point x_1 is very close to zero, the probability that the height at the next point $x_2=x_1+1$ has the same sign as that of the height at the initial point (this is the first value of the measured "no zero crossing probability") is actually close to 0.5 in all the numerical simulations—for h_1 slightly above zero, the probability of h_2 remaining positive is close to 0.5 because, as discussed in Sec. II, the height difference $s_1=h_2-h_1$ is a Gaussian random variable with zero mean.

Our numerical results (such as those shown in Fig. 4) suggest that for a fixed value of $y=w/W(L)$, the scaling functions $f_{FIC}(u,\delta x/L,w)$ for different values of $\delta x/L$ differ from one another mainly by an overall numerical prefactor that decreases as the value of $\delta x/L$ is reduced. This is why the analytic results for the survival probability show reasonable agreement with the numerical data (as shown in Fig. 8) when the former are multiplied by a suitable numerical factor. An approximate analytic estimate of this numerical factor may be obtained in the following way. Using the statistical properties of the height difference variables $\{s_i\}$ mentioned in Sec. II, it is easy to show that for $L\gg 1$, the probability that the height h_2 at lattice site 2 has the same sign as that of h_1, the height at site 1, is given by $0.5[1+\mathrm{erf}(h_1/\sqrt{2})]$. The "one-step" FIC survival probability for discrete sampling with $\delta x=1$ is then given by

$$Q_{1d}(w,L)=Q_{FIC}(x=1,L,\delta x=1,w)=0.5\left(1+\frac{\int_0^w dh_1\,\exp(-h_1^2/2W)\mathrm{erf}(h_1/\sqrt{2})}{\int_0^w dh_1\,\exp(-h_1^2/2W)}\right), \tag{70}$$

where $W(L)=\sqrt{L/12}$ is the steady-state width of the inter-

face. For $w \ll W(L)$, this becomes a function of w only:

$$Q_{1d}(w) = 0.5[1 + \mathrm{erf}(w/\sqrt{2}) - \sqrt{2/\pi}(1 - e^{-w^2/2})/w]. \quad (71)$$

As expected, $Q_{1d}(w)$ goes to 0.5 as $w \to 0$. Our numerical results for $Q_{1d}(w)$ are in good agreement with this analytic prediction. The one-step FIC survival probability in the continuum limit may be obtained by setting $x=1$ in Eq. (19), integrating $Q(x=1, L|h_0)P_{st}(h_0)$ over h_0 between 0 and w, and dividing by $\int_0^w P_{st}(h_0)dh_0$ for normalization. For $w \ll W(L)$, $L \gg 1$, this leads to the result

$$Q_{1c}(w) = Q_{FIC}(x=1, L, \delta x = 0, w) = \mathrm{erf}(w/\sqrt{2}) - \sqrt{2/\pi}(1 - e^{-w^2/2})/w = 2Q_{1d}(w) - 1. \quad (72)$$

Thus, $Q_{1c}(w)$ goes to zero as $w \to 0$, as expected. However, both $Q_{1d}(w)$ and $Q_{1c}(w)$ approach unity for $L \gg 1$, $w \gg 1$, $w/W(L) \to 0$, indicating that the numerical and analytic results would agree with each other in this limit. For $w/W(L)=0.02$, $L=10^4$ (the values for which numerical results are shown in Fig. 8), the values of the one-step survival probabilities are $Q_{1d}=0.612$ and $Q_{1c}=0.224$. The ratio of these two number is 2.73, which is slightly smaller than the empirical multiplicative factor used in Fig. 8 to bring the analytic result for the FIC survival probability in approximate agreement with the numerical data. This difference reflects the fact that the empirical value used in Fig. 8 was obtained by considering the analytic and numerical results for a range of values of x, whereas the analytic estimate of the multiplicative factor is obtained by considering only one point.

IV. SUMMARY AND DISCUSSIONS

In this paper, we have presented analytic and numerical results for the spatial survival probabilities for 1D EW interfaces in the steady state. In one dimension the same steady-state results also hold for the KPZ interface. We have studied both the steady-state and the FIC survival probabilities. The numerical results show that these survival probabilities exhibit simple scaling behavior as functions of the system size and the sampling interval used in the measurement. In the analytic work, we have used a "deterministic" approximation to obtain closed-form expressions for these scaling functions from an exact path integral treatment of a mapping of the problem to 1D Brownian motion. The analytic results show fairly good agreement with the numerical data without having to use any adjustable parameter. The remaining differences between the analytic and numerical results may be attributed to (a) the use of the deterministic approximation in obtaining the analytic results and (b) the use of a finite sampling interval in the numerical calculations. The effect of discrete sampling is small in the case of the steady-state survival probability. For the FIC survival probability, the dependence of the numerical results on the value of the sampling interval used in the measurement is approximately described by an overall multiplicative factor. The value of this multiplicative factor can be estimated analytically by considering the one-step survival probability. Further analytic work on the dependence of the survival probabilities on the sampling interval would be interesting and useful, especially because measurements of these probabilities in simulations and experiments always involve discrete sampling. While some progress in this direction has been made [16], a complete analysis of the effects of discrete sampling remains a challenging theoretical problem.

On the experimental side, fluctuating steps on a vicinal surface provide a physical realization of 1D EW interfaces if the kinetics is dominated by attachment/detachment processes [15]. While experimental studies of temporal persistence and survival probabilities have been carried out [6–9] for this system, we are not aware of any experimental investigation of spatial first-passage properties of fluctuating steps. Such investigations would be most welcome. In other experimental systems such as combustion fronts in paper which also involve 1D interfaces described by the EW or the KPZ equation, the spatial persistence has been recently investigated [13]. It would be interesting to see if our theoretical predictions on the spatial survival probability can also be verified experimentally in such systems.

APPENDIX: FINITE 1D EW INTERFACES WITH PERIODIC BOUNDARY CONDITION

Consider the EW equation (1) on a finite line of size L with periodic boundary condition, $h(x+L,t)=h(x,t)$. Since $h(x,t)$ is a periodic function, one can decompose it into a Fourier series, $h(x,t)=\Sigma_k \tilde{h}(k,t)e^{ikx}$ where $k=2\pi m/L$ with $m=0, \pm 1, \pm 2, \ldots$. Thus

$$h(x,t) = \sum_{m=-\infty}^{\infty} \tilde{h}(m,t)e^{2\pi i m x/L}, \quad (A1)$$

where the Fourier coefficients $\tilde{h}(m,t)$ are given by the inversion formula,

$$\tilde{h}(m,t) = \frac{1}{L}\int_0^L h(x,t)e^{-2\pi i m x/L}dx. \quad (A2)$$

Substituting Eq. (A1) in the EW equation (1) one gets

$$\partial_t \tilde{h}(m,t) = -\frac{4\pi^2 m^2}{L^2}\Gamma \tilde{h}(m,t) + \tilde{\eta}(m,t), \quad (A3)$$

for all $m \neq 0$, where $\langle \tilde{\eta}(m,t) \rangle = 0$ and $\langle \tilde{\eta}(m,t)\tilde{\eta}(m',t') = (2D'/L)\delta_{m+m',0}$ with $\delta_{m,n}$ being the Kronecker delta function. Note that for $m=0$, $\tilde{h}(0,t)=0$ at all t, because of the sum rule, $\int_0^L h(x,t)dx=0$. Solving Eq. (A3) with initial condition $\tilde{h}(m,0)=0$, we get for $m \neq 0$,

$$\tilde{h}(m,t) = \int_0^t \exp[-4\pi^2 m^2 \Gamma (t-t')/L^2]\tilde{\eta}(m,t')dt'. \quad (A4)$$

Using Eq. (A4) and the properties of the noise, one can easily compute the two-point equal time correlation function and we get

$$\langle \tilde{h}(m_1,t)\tilde{h}(m_2,t)\rangle = \frac{2D'}{\Gamma L}\frac{L^2}{8\pi^2 m_1^2} \times[1-\exp(-8\pi^2 m_1^2 \Gamma t/L^2)]\delta_{m_1+m_2,0}. \quad \text{(A5)}$$

This gives the two-point correlation function in real space,

$$\langle h(x_1,t)h(x_2,t)\rangle = \frac{2D'}{\Gamma L}\sum_{m_1\neq 0}\frac{L^2}{8\pi^2 m_1^2}[1-\exp(-8\pi^2 m_1^2\Gamma t/L^2)] \times\exp[2\pi i m(x_1-x_2)/L]. \quad \text{(A6)}$$

Note that the sum in Eq. (A6) runs from $m=-\infty$ to $m=\infty$ but does not include the $m=0$ term, since we have used the fact that $\tilde{h}(m=0,t)=0$. In particular, putting $x_1=x_2=x$, we get the on-site variance, which becomes independent of x as expected, due to the translational invariance. This gives

$$\langle h^2(0)\rangle = \frac{2D'}{\Gamma L}\sum_{m_1\neq 0}\frac{L^2}{8\pi^2 m_1^2}[1-\exp(-8\pi^2 m_1^2\Gamma t/L^2)]. \quad \text{(A7)}$$

In the stationary limit ($t\to\infty$), one gets from Eq. (A7)

$$\langle h^2(0)\rangle = \frac{D'L}{2\pi^2\Gamma}\sum_{m=1}^{\infty}\frac{1}{m^2}. \quad \text{(A8)}$$

Using the identity, $\Sigma_{m=1}^{\infty}=\pi^2/6$, we get the formula for the on-site variance in the stationary limit,

$$\langle h^2(0)\rangle = \frac{D'}{12\Gamma}L = \frac{DL}{6}, \quad \text{(A9)}$$

where $D=D'/2\Gamma$. Since Eq. (1) is linear, it follows then that the single site height distribution is a pure Gaussian at all times. In particular, the stationary distribution is given by

$$P_{\rm st}(h_0) = \frac{1}{\sqrt{2\pi\langle h^2(0)\rangle}}\exp[-h_0^2/2\langle h^2(0)\rangle], \quad \text{(A10)}$$

where $\langle h^2(0)\rangle$ is given in Eq. (A9).

[1] For a review on temporal persistence, see S. N. Majumdar, Curr. Sci. **77**, 370 (1999).
[2] J. Krug, H. Kallabis, S. N. Majumdar, S. J. Cornell, A. J. Bray, and C. Sire, Phys. Rev. E **56**, 2702 (1997).
[3] H. Kallabis and J. Krug, Europhys. Lett. **45**, 20 (1999).
[4] M. Constantin, C. Dasgupta, P. Punyindu Chatraphorn, Satya N. Majumdar, and S. Das Sarma, Phys. Rev. E **69**, 061608 (2004).
[5] C. Dasgupta, M. Constantin, S. Das Sarma, and Satya N. Majumdar, Phys. Rev. E **69**, 022101 (2004).
[6] D. B. Dougherty, I. Lyubinetsky, E. D. Williams, M. Constantin, C. Dasgupta, and S. Das Sarma, Phys. Rev. Lett. **89**, 136102 (2002).
[7] D. B. Dougherty, O. Bondarchuk, M. Degawa, and E. D. Williams, Surf. Sci. **527**, L213 (2003).
[8] O. Bondarchuk, D. B. Dougherty, M. Degawa, E. D. Williams, M. Constantin, C. Dasgupta, and S. Das Sarma, Phys. Rev. B **71**, 045426 (2005).
[9] D. B. Dougherty, C. Tao, O. Bondarchuk, W. G. Cullen, E. D. Williams, M. Constantin, C. Dasgupta, and S. Das Sarma, Phys. Rev. E **71**, 021602 (2005).
[10] S. N. Majumdar and A. J. Bray, Phys. Rev. Lett. **86**, 3700 (2001).
[11] M. Constantin, S. Das Sarma, and C. Dasgupta, Phys. Rev. E **69**, 051603 (2004).
[12] M. Kardar, G. Parisi, and Y.-C. Zhang, Phys. Rev. Lett. **56**, 889 (1986).
[13] J. Merikoski, J. Maunuksela, M. Myllys, J. Timonen, and M. J. Alava, Phys. Rev. Lett. **90**, 024501 (2003).
[14] S. F. Edwards and D. R. Wilkinson, Proc. R. Soc. London, Ser. A **381**, 17 (1982).
[15] N. C. Bartelt, J. L. Golding, T. L. Einstein, and E. D. Williams, Surf. Sci. **273**, 252 (1992).
[16] S. N. Majumdar, A. J. Bray, and G. C. M. A. Ehrhardt, Phys. Rev. E **64**, 015101(R) (2001); G. C. M. A. Ehrhardt, A. J. Bray, and S. N. Majumdar, *ibid.* **65**, 041102 (2002).
[17] W. H. Press *et al.*, *Numerical Recipes* (Cambridge University Press, Cambridge, 1989).
[18] S. N. Majumdar and A. Comtet, Phys. Rev. Lett. **92**, 225501 (2004).
[19] S. N. Majumdar and A. Comtet, J. Stat. Phys. **119**, 777 (2005).
[20] A. L. Barabasi and H. E. Stanley, *Fractal Concepts in Surface Growth* (Cambridge University Press, Cambridge, England, 1995); T. Halpin-Healy and Y.-C. Zhang, Phys. Rep. **254**, 215 (1995). J. Krug, Adv. Phys. **46**, 139 (1997).
[21] G. Foltin, K. Oerding, Z. Racz, R. L. Workman, and R. K. P. Zia, Phys. Rev. E **50**, R639 (1994).
[22] S. Redner, *A Guide to First-passage Processes* (Cambridge University Press, Cambridge, 2001).
[23] T. W. Burkhardt, J. Phys. A **26**, L1157 (1993).
[24] D. A. Darling, Ann. Prob. **11**, 803 (1983).
[25] G. Louchard, J. Appl. Probab. **21**, 479 (1984).
[26] L. Takacs, Adv. Appl. Probab. **23**, 557 (1991); J. Appl. Probab. **32**, 375 (1995).
[27] P. Flajolet, P. Poblete, and A. Viola, Algorithmica **22**, 490 (1998); P. Flajolet and G. Louchard, *ibid.* **31**, 361 (2001).
[28] M. Perman and J. A. Wellner, Ann. Appl. Probab. **6**, 1091 (1996).
[29] C. L. Mallows and J. Riordan, Bull. Am. Math. Soc. **74**, 92 (1968); E. M. Wright, J. Graph Theory **1**, 317 (1977); I. Gessel, B. E. Sagan, and Y.-N. Yeh, *ibid.* **19**, 435 (1995).
[30] C. Richard, J. Stat. Phys. **108**, 459 (2002); M. J. Kearney, J. Phys. A **37**, 8421 (2004).
[31] M. Abramowitz and I. A. Stegun, *Handbook of Mathematical Functions* (Dover, New York, 1973).